

MODULAR JET AND PROPELLER ENGINE – PART II: INTEGRATED DESIGN PROCESS AND DESIGN SPACE ASSESSMENT

Tomasz Matuschek[1], Tom Otten[1], Jannik Häßy[1],
Robin Brakmann[2], Julie Frank[2] & Patrick Wehrel[1]

[1]German Aerospace Center (DLR), Institute of Propulsion Technology, Engine department
[2] German Aerospace Center (DLR), Institute of Propulsion Technology, Turbine department

Abstract

Small turbojet engines offer compact integration and high specific thrust, but show low propulsive efficiency at low and medium flight speeds. The Modular Jet and Propeller Engine (MOJO) concept addresses this limitation by using a small turbojet as an unchanged gas generator and adding a modular power turbine and propeller extension. Building on Part I, this paper investigates the coupled design space of this extension.

An integrated conceptual design process combines engine performance simulation, preliminary propeller design, power turbine design and component mass estimation. It is applied to geared and direct-drive MOJO configurations to assess the interaction between propeller diameter, rotational speed, tip Mach number, nozzle pressure ratio, transmission concept and extension mass.

The results show that the geared configuration provides robust design freedom through shaft-speed decoupling, while the direct-drive configuration is more compact but strongly constrained by fixed shaft-speed coupling. Target-thrust studies indicate that candidates selected from the full-load design space do not necessarily provide the lowest fuel consumption at lower required thrust levels, highlighting the need to evaluate thrust-specific fuel consumption together with geometric feasibility, extension mass and thrust margin.

Keywords: Propulsion, Turbojet, Turboprop, Conceptual Design

1. Introduction and Motivation

Small unmanned aerial vehicles increasingly require propulsion systems that combine compact integration and high thrust-to-weight ratio with improved fuel efficiency at low and medium flight speeds [1]. Small turbojet engines are attractive for high-speed operation due to their compact architecture and high specific thrust, but their high jet velocity leads to poor propulsive efficiency in slower flight regimes. Propeller-based propulsion systems offer higher propulsive efficiency at these operating points, but are limited by diameter, integration and tip-speed constraints.

Motivated by this trade-off, the Modular Jet and Propeller Engine (MOJO) concept uses a small turbojet as an unchanged gas generator and adds a modular power turbine and propeller unit downstream of the core turbine. The general concept, baseline turbojet model and first retrofit configurations have been introduced in Part I [2] of this two-part contribution. Part I showed that both geared and direct-drive propeller retrofit configurations can substantially reduce fuel consumption compared with the baseline turbojet, while also revealing architectural differences between both concepts.

Building on these initial studies, the present paper extends the analysis from selected design points to a systematic assessment of the coupled design space of the MOJO extension. The study investigates how power turbine, propeller and transmission parameters interact under geared and direct-drive assumptions, while preserving the common gas-generator concept introduced in Part I.

The paper is structured as follows: Section 2 formulates the design problem and research objectives. Section 3 introduces the integrated design methodology, including engine performance simulation, propeller design, turbine design and mass estimation. Section 4 applies the process to geared and direct-drive MOJO configurations and discusses full-load design spaces, target-thrust adaptation and constrained architecture comparison.

2. Design Problem and Research Objectives

The design of a modular turboprop extension is governed by strong interdependencies between gas-generator operation, power turbine design, propeller aerodynamics, transmission concept and geometric integration constraints. A change in one design parameter typically affects several subsystems simultaneously. Propeller diameter, rotational speed and tip Mach number influence propeller efficiency, while the required shaft power and turbine loading determine power turbine speed, geometry and efficiency. In geared configurations, the gearbox introduces an additional degree of freedom by decoupling turbine and propeller speed, but also adds mass and integration complexity. In direct-drive configurations, the gearbox is removed, but power turbine and propeller must operate at the same shaft speed.

Part I [2] demonstrated the general feasibility of the MOJO retrofit concept and compared initial geared and direct-drive configurations. The geared configuration was found to provide the more robust performance solution due to the decoupling of turbine and propeller speed, whereas the direct-drive configuration remained potentially attractive for compact installations because it eliminates the gearbox and allows smaller propeller diameters where these are imposed by airframe integration constraints. However, the initial studies were based on selected design points and therefore do not provide a systematic analysis of the feasible design space.

At an early design stage, platform-specific constraints such as required thrust, allowable propeller diameter, acceptable extension mass or installation volume are often not yet fixed. A single design-point comparison is therefore insufficient to support architectural decisions. Instead, the relevant design space must be explored in order to identify how performance and feasibility change with diameter, tip Mach number, gear ratio, power turbine loading, nozzle pressure ratio and gas-generator power setting.

The objective of this paper is therefore to establish and apply an integrated conceptual design process for the MOJO extension. The study focuses on the dominant trade-offs between propeller efficiency, diameter, rotational speed, tip Mach number and estimated extension mass, and compares how geared and direct-drive configurations differ in terms of design freedom, feasibility boundaries and target-thrust adaptation. Particular attention is given to the question under which generic thrust and diameter constraints a direct-drive configuration can remain competitive despite the expected penalties associated with fixed shaft-speed coupling.

The resulting assessment is not intended to define a final aircraft-specific optimum. Instead, it provides a structured basis for understanding architecture-specific trends and for identifying promising regions of the design space that can later be refined in platform-coupled studies.

3. Integrated Design Methodology

The integrated design methodology evaluates the coupled design space of the MOJO turboprop extension at conceptual design level. It combines engine performance simulation, preliminary propeller design, power turbine efficiency estimation, component geometry generation and mass estimation. The process is intended to identify dominant trends and feasibility constraints rather than to generate fully detailed component designs for every investigated design point.

3.1 Overall Process Chain

The integrated process is established within the modular software environment *GTlab* [3,4] and is illustrated in Figure 1. For each candidate, the flight condition, gas-generator load setting and architecture-specific design variables are prescribed. The performance model evaluates the thermodynamic state of the fixed gas generator and the power available to the modular extension.

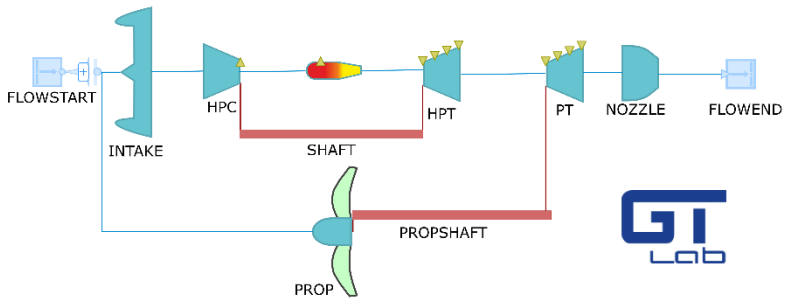


Figure 1 – Thermodynamic performance model of the MOJO configuration.

The propeller is designed with *PROPSTER* [5,6] and iterated with the performance model through the resulting propeller efficiency. The power turbine efficiency used in the design-space studies is estimated by a conceptual efficiency correlation [7]. Higher-fidelity mean-line and through-flow turbine methods [8-10] are applied only to selected representative designs in order to calibrate and verify the correlation-based assumptions. Accordingly, the turbine design and map-generation steps shown in Figure 2 should be interpreted as supporting verification steps rather than as a fully automated detailed design loop for every parameter-study member.

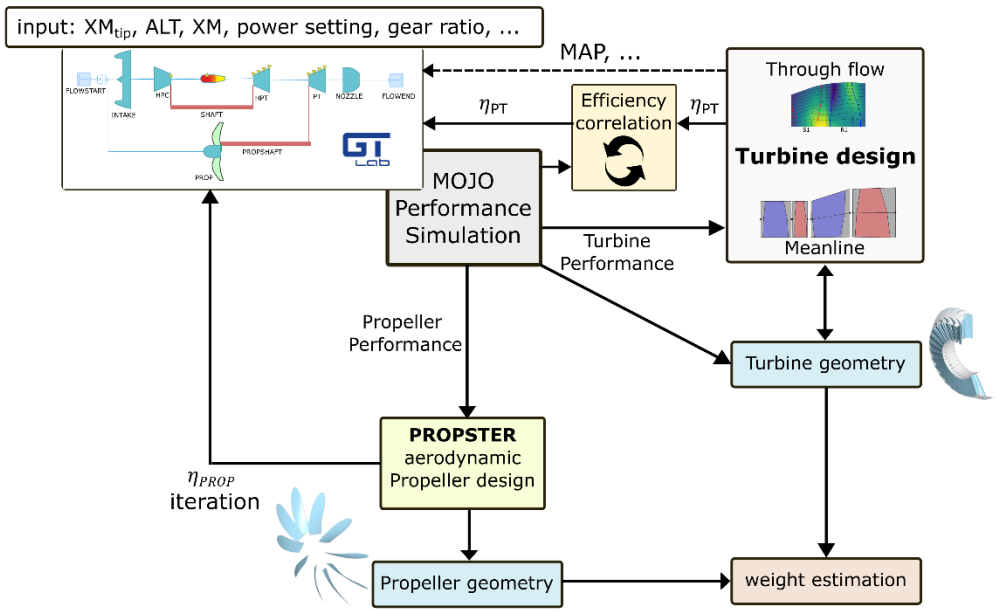


Figure 2 – Illustration of the integrated design process for the Modular Jet and Propeller Engine.

The following subsections summarize the main elements of the process chain: performance simulation, propeller design, turbine design, as well as geometry and mass estimation.

3.2 Performance Simulation

The performance simulation is implemented in *GTlab* [3,4] and uses the baseline turbojet model introduced in Part I [2] as a fixed gas generator. The present paper focuses on the additional MOJO extension downstream of the core turbine, consisting of the power turbine (PT), propeller and, for the geared configuration, the gearbox. For each design point, the flight condition, gas-generator load setting and architecture-specific design variables are prescribed. The performance model determines the thermodynamic state upstream of the power turbine, the extracted shaft power and the residual nozzle thrust.

The coupled design problem is formulated as an equation system summarized in Table 1. The propeller power coefficient C_P and the power turbine loading coefficient Ψ_{PT} are used as central coupling parameters:

$$C_P = \frac{P}{\rho \cdot {n_{PROP}}^3 \cdot D^5} \tag{1}$$

$$\Psi_{PT} = \frac{\Delta h_{PT}}{{U_m}^2} \quad \text{with } U_m = 2\pi \cdot n_{PT} \cdot R_{m,out} \tag{2}$$

Here, P is the propeller shaft power, ρ the freestream density, n_{Prop} the propeller rotational speed, D the propeller diameter, Δh_{PT} the specific total enthalpy difference across the power turbine, and U_m the circumferential blade speed at the rotor outlet. The latter is calculated from the power turbine rotational speed n_{PT} and the mean rotor outlet radius $R_{m,out}$. The propeller efficiency is iterated with the preliminary propeller design described in Section 3.3 as well as in Part I [2]. Table 1 summarizes the resulting equation systems for the two architectures.

Table 1 – MOJO equation system, architecture variables and boundary conditions.

Boundary conditions	*ALT*, *XM*, N_{rel}, i_{gear} (const. for direct), …
Architecture variable	*NPR* (direct), i_{gear} (geared)
MOJO equation system to be solved	
Independents	**Dependents**
Propeller C_P	Nozzle pressure ratio *NPR* (const. for geared)
Propeller Diameter *D*	Propeller tip speed XM_{tip}
Propeller shaft speed n_{Prop}	Power turbine loading Ψ_{PT}
Propeller efficiency η_{Prop}	Iterated with *PROPSTER* (see Section 3.3)
$(R_{hub}/R_{tip})_{in}$	$R_{tip,in}$ (direct), $R_{hub,in}$ (geared)
$(R_{hub}/R_{tip})_{out}$	$R_{tip,out}$ (direct), $R_{hub,out}$ (geared)

The main architecture-specific differences are the shaft-speed coupling and the turbine annulus definition. In the geared configuration, the gearbox decouples propeller and power turbine speed; the gear ratio i_{gear} is therefore used as an architecture variable and the remaining nozzle pressure ratio is kept close to its minimum value. In the direct-drive configuration, both components rotate at the same shaft speed. The remaining nozzle pressure ratio *NPR* is therefore introduced as a design variable to adjust power extraction and turbine speed. Furthermore, the direct-drive turbine is sized by prescribing the tip radius at inlet and outlet in order to maximize the radial position of the turbine stage, whereas the geared configuration uses a hub-radius-based sizing approach for compatibility with the gas-generator turbine exit.

3.3 Aerodynamic Propeller Design

The preliminary propeller design is performed using *PROPSTER*, an in-house propeller design and analysis tool developed at DLR's Institute of Propulsion Technology [5,6]. It combines blade-element-based aerodynamic modelling with design methods based on blade element momentum and vortex theory. The tool determines the propeller geometry and aerodynamic performance based on prescribed flight conditions, propeller diameter, rotational speed, blade number, airfoil distribution and either required thrust or shaft power.

In the present study, a fixed NACA-based airfoil family is used and the radial design lift-coefficient distribution is prescribed as constant with $C_L = 0.5$ along the blade span. The resulting propeller efficiency is iterated with the engine performance model as described in Section 3.2. Compressibility effects are considered using Mach-dependent airfoil polar data. In addition, the sweep angle distribution can be varied in *PROPSTER* and is used to account for the reduction of the effective inflow Mach number experienced by the blade sections.

3.4 Power Turbine Design

The power turbine design process combines a correlation-based efficiency estimation for large design-space studies with higher-fidelity turbine design methods. Within the parametric studies, the power turbine efficiency is estimated using the conceptual efficiency correlation introduced in [7]. This allows a large number of design candidates to be evaluated efficiently while retaining the main dependencies on turbine loading, flow coefficient and geometry.

A detailed geometry is generated for selected designs from the engine level model by using the 1D meanline program *PrEDiCT* [8,9]. The flow field within the turbine is then calculated with the throughflow solver *SLC4T* [9,10] in order to verify the plausibility of the resulting geometry and efficiency assumptions. An additional description of the process and models is provided in Part I [2] of this paper.

In the present study, this detailed turbine design and map-generation procedure is applied only to selected representative designs. The complete design-space exploration relies on the calibrated correlation-based efficiency estimate. The detailed turbine calculations therefore serve as verification and calibration steps, while the performance-based turbine geometry remains sufficiently accurate for comparing trends within the parametric studies.

3.5 Geometry and Mass Estimation Methods

Based on the converged performance and propeller design results, preliminary geometries are

generated for the power turbine and propeller. The power turbine geometry is obtained from the performance-based sketching approach and provides the annulus dimensions required for mass estimation. Selected representative turbine designs are additionally verified using meanline and through-flow methods. However, this higher-fidelity verification is not performed for every member of the parametric studies.

The component masses are estimated from the resulting geometries. Turbomachinery masses are calculated using the knowledge-based geometry and mass estimation methods from [11], while gearbox mass is estimated with the correlation from [12] using transmitted power, gear ratio and number of gear stages. The propeller mass is predicted by means of an empirical approach that is based on the propeller diameter, the number of blades, sweep angle, activity factor, maximum circumferential tip speed, and the maximum shaft power. The methodology was originally published by [13] and adapted in [14] by introducing a calibrated technology factor that reflects the level of modern propellers. The extension mass is defined as

$$W_{\mathrm{Ext}} = W_{\mathrm{PT}} + W_{\mathrm{Prop}} + W_{\mathrm{Gear}} \tag{3}$$

with $W_{\mathrm{Gear}} = 0$ for the direct-drive configuration. W_{Ext} is therefore the estimated mass of the added MOJO extension. At this conceptual stage, it is mainly used to compare trends within one architecture. Direct mass estimations remain uncertain because bearing loads, support structures, and detailed propeller integration are not yet fully captured.

4. Results and Discussion

The following section applies the integrated design methodology to the coupled design space of the MOJO extension. The intention is not to define a final aircraft-specific optimum, but to identify the dominant trends and constraints that result from the interaction of power turbine design, propeller aerodynamics and transmission concept. The results are first discussed for the geared and direct-drive full-load design spaces and are then extended to target-thrust operation and constrained architecture comparison.

4.1 Study Setup and Common Assumptions

All design studies are based on the same fixed gas generator introduced in Part I [2]. The investigated design freedom is therefore limited to the modular MOJO extension downstream of the core turbine, consisting of the power turbine, propeller and, for the geared configuration, the gearbox. Within this paper, the studies are evaluated at sea-level altitude ALT = 0 m and a flight Mach number of XM = 0.4, representing a low-altitude operating condition where propeller-based propulsion is expected to provide a relevant efficiency benefit.

The following results compare geared and direct-drive configurations under architecture-specific but consistent modelling assumptions. In the geared configuration, the gearbox decouples power turbine and propeller speed. The gear ratio i_{gear} is therefore available as an additional design variable, while the remaining nozzle pressure ratio *NPR* is kept close to its minimum value. Since the rear-mounted gearbox arrangement complicates efficient utilization of the residual nozzle thrust, a reduced nozzle gross thrust coefficient is assumed.

In the direct-drive configuration, the propeller and power turbine rotate at the same shaft speed. The remaining nozzle pressure ratio *NPR* is therefore introduced as an additional design variable to adjust power extraction and shaft speed. To make this configuration feasible within the investigated diameter range, the direct-drive case is evaluated with a more aggressive turbine and propeller parametrization, including a higher turbine loading Ψ_{PT} and a tip-radius-based turbine sizing approach. These architecture-specific assumptions are summarized in Table 2.

The evaluated quantities are selected to capture both performance and integration-relevant effects. Thrust and thrust specific fuel consumption (*TSFC*) describe the propulsion-system performance, while propeller diameter, tip Mach number, chord ratio and estimated extension mass characterize geometric feasibility and integration penalties. The chord ratio *c/D* at $x = r/R = 0.75$ is used as a simplified propeller plausibility criterion, with values between 0.05 and 0.10 considered as the practical design band in this study.

Table 2 summarizes the main assumptions and varied design parameters used for the following design-space studies.

Table 2 – Main assumptions and varied design parameters used for the design-space studies, all given values are for the design point, which represents full-load (maximum thrust).

Parameter / assumption	**Geared drive**	**Direct drive**
Flight condition	$ALT = 0$ m, $XM = 0.4$	
PT inlet/outlet Mach assumption	$XM_{PT,in}$, $XM_{PT,out} = 0.5$	
Propeller blade number	$B = 8$, adjusted later	
Chord ratio validity range	$c/D\|_{x=0.75} = 0.05 – 0.10$	
Tip Mach constraint	$XM_{tip} < 1.4$	
Propeller airfoil	NACA 16 series	
Pressure loss inter turbine duct	0 %	3 %
Power turbine loading	$\Psi_{PT} = 2.0$	$\Psi_{PT} = 2.5$
Power turbine sizing	$R_{hub} = 0.0356$ m	$R_{tip} = 0.117$ m
Nozzle gross thrust coefficient	$GTC = 0.5$	$GTC = 1.0$
Nozzle pressure ratio	$NPR = 1.01$	varied
Transmission efficiency	98 %	99 %
Sweep assumption [15,16]	SR3-based, tip sweep 12°	SR3-based, tip sweep 45°
Primary design variables	XM_{tip}, N_{rel}, i_{gear}	XM_{tip}, N_{rel}, NPR
Evaluated quantities	FN, $TSFC$, D, η_{Prop}, W_{ext}	

The following sections first consider the full-load design spaces of both architectures. This separates the architectural design freedom from the later target-thrust evaluation and provides a reference for assessing whether a design optimized for maximum available thrust also represents a suitable candidate for a specific lower thrust requirement.

4.2 Geared-drive Design Space

The geared configuration is first investigated at full-load operation in order to identify the design freedom introduced by the gearbox. Since propeller and power turbine speed are decoupled, the gear ratio can be selected such that the propeller operates at a favorable combination of diameter, rotational speed and tip Mach number, while the power turbine remains within the assumed loading constraint.

Figure 3 shows the resulting geared-drive design space as a function of propeller diameter and propeller rotational speed. The background color represents the estimated extension mass, while contour lines indicate propeller efficiency, tip Mach number and the chord ratio c/D at 75 % span. The red line marks the maximum propeller efficiency for each diameter and is used as a full-load reference corridor for the following analysis.

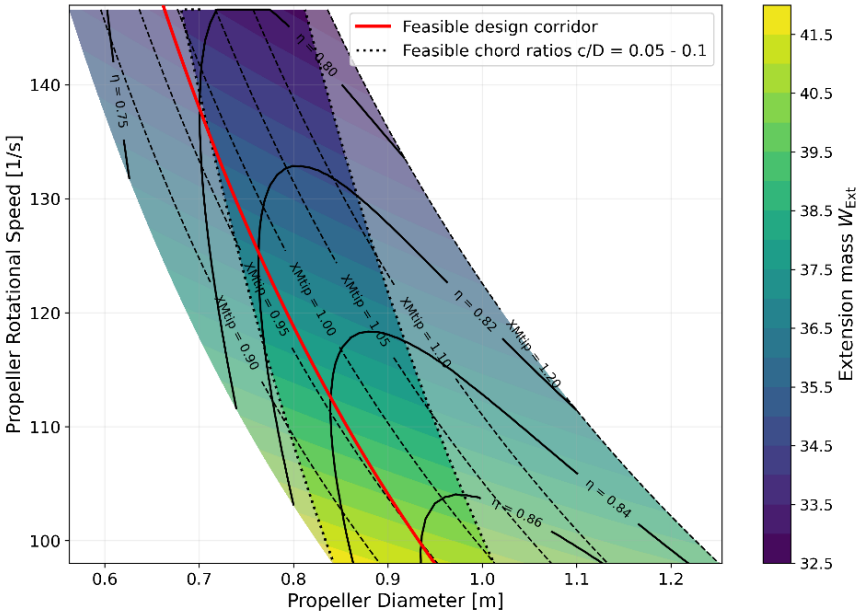


Figure 3 – Geared-drive full-load design space.

The results indicate that favorable geared-drive designs are not concentrated in a single isolated optimum, but form a continuous corridor in the diameter-speed plane. Along this corridor, increasing propeller diameter generally reduces disk loading and improves propeller efficiency. At the same time, larger diameters and the associated gearbox design introduce integration and mass penalties. The geared architecture therefore provides a family of efficient full-load candidates, from which a design can be selected depending on the available installation diameter and acceptable extension mass.

The orientation of the efficiency contours indicates that this corridor approximately follows a line of comparable propeller tip Mach number, with the optimum shifting toward lower rotational speed as diameter increases. The exact position of the corridor depends on the selected propeller parametrization, including airfoil family, sweep distribution and loading assumptions. The red line should therefore be interpreted as the optimum corridor for the selected design assumptions, not as a universal propeller optimum.

The chord ratio contours provide an additional plausibility check for the propeller geometry. Designs outside the selected chord ratio band may still be numerically feasible in the integrated performance model, but would require a modified propeller layout, for example by changing blade number or loading distribution. This criterion is therefore used to distinguish between performance-feasible and aerodynamically plausible candidates.

The geared-drive design space illustrates the main benefit of speed decoupling: propeller aerodynamic constraints can be addressed by selecting a suitable combination of diameter, tip Mach number and gear ratio. The resulting full-load corridor serves as a reference for the subsequent target-thrust analysis, where the most efficient design at maximum thrust is compared with candidates optimized for a lower thrust requirement.

4.3 Direct-drive Design Space

The direct-drive configuration is investigated next in order to assess how the design space changes when the gearbox degree of freedom is removed. In contrast to the geared configuration, propeller and power turbine speed are directly coupled. As a result, propeller diameter, tip Mach number, power turbine loading and remaining nozzle pressure ratio become strongly interdependent. The design problem therefore changes from selecting a suitable gear ratio to finding a feasible compromise between turbine and propeller requirements.

Figure 4 shows the direct-drive full-load design space as a function of design tip Mach number XM_{tip} and remaining nozzle pressure ratio *NPR*. The background color represents *TSFC* at full-load operation, while contour lines indicate the resulting propeller diameter. The chord ratio validity band is included as a geometric plausibility criterion, and non-converged regions are excluded from the feasible design space.

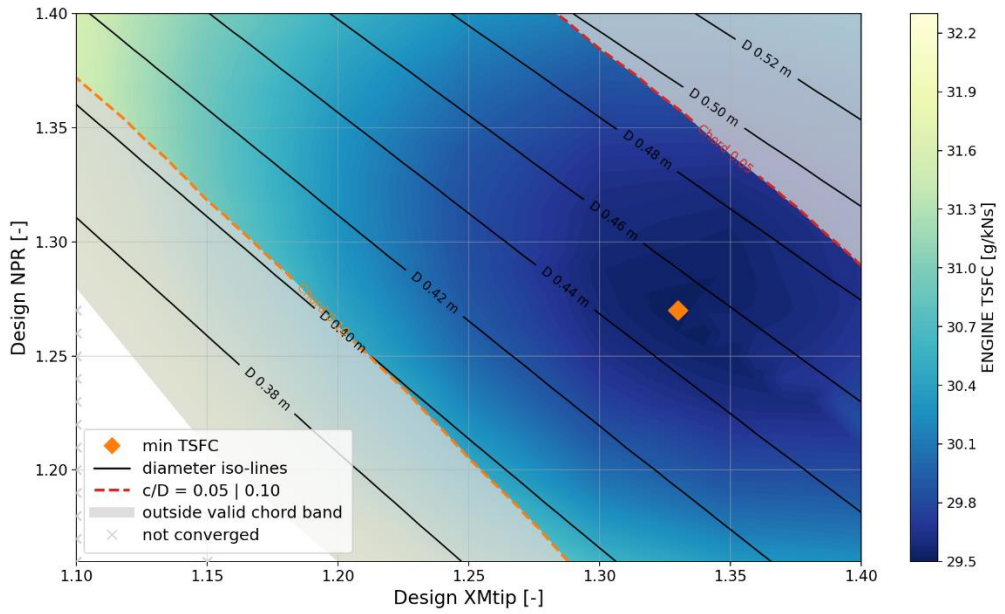


Figure 4 – Direct-drive full-load design space.

Compared with the geared configuration, the feasible design space is substantially more constrained. Compact propeller diameters require comparatively high design tip Mach numbers, while larger diameters can only be reached by reducing the coupled shaft speed. In the direct-drive architecture, this is achieved by increasing the remaining nozzle pressure ratio, which reduces power extraction across the power turbine and shifts the operating point toward lower rotational speed.

The resulting *TSFC* field shows a distinct minimum within the investigated parameter range. In the present study, the full-load minimum occurs at approximately $NPR = 1.27$ and $XM_{tip} = 1.33$. This optimum is located at an intermediate combination of design tip Mach number and nozzle pressure ratio, indicating that neither maximum power extraction nor maximum residual jet thrust is favorable. Instead, the direct-drive optimum results from a balance between propeller efficiency, shaft power extraction, residual jet thrust and geometric feasibility.

The chord ratio contours show that the aerodynamically plausible region remains sensitive to the selected blade number and loading assumptions. Propeller geometry refinements can therefore improve the feasibility of individual candidates.

The direct-drive design space highlights the main architectural trade-off of this configuration. Eliminating the gearbox reduces mechanical complexity and avoids gearbox-related mass and integration challenges, but it also removes the primary degree of freedom used to place the propeller in a favorable operating region. Consequently, the direct-drive architecture requires a more aggressive turbine and propeller parametrization and remains more sensitive to diameter, tip Mach number, nozzle pressure ratio and chord ratio constraints. As for the geared configuration, the full-load optimum provides an important reference point, but is not necessarily identical to the best design for a specified lower target thrust.

4.4 Target-thrust Design Adaptation

The full-load design spaces discussed in the previous sections provide useful reference points for both architectures. However, a design that is favorable at maximum available thrust is not necessarily the most fuel-efficient candidate when the propulsion system is evaluated at a specific lower thrust requirement. In a clean-sheet design, such operating points could also be addressed by selecting a smaller gas generator operated closer to full-load. This option is deliberately not considered here, since the MOJO concept follows a modular engine-family approach in which existing small turbojet cores are retained and adapted to different thrust requirements by means of the downstream turboprop extension. This distinction is particularly relevant because different aircraft platforms or mission segments may require different thrust levels while still relying on the same baseline gas generator.

In this section, the analysis is therefore extended from full-load operation to an exemplary target-thrust condition of $FN_{target} = 1000$ N. This value is used as a representative requirement to investigate how the design parameters can be adapted when fuel consumption at a specified operating point becomes the primary objective. The target-thrust studies do not replace the full-load analysis, but complement it: the full-load design space indicates the maximum thrust capability and the general feasibility of an architecture, while the target-thrust analysis shows whether a different design point can reduce *TSFC* at a mission-relevant operating condition.

Adapting a design to a lower target thrust introduces an additional trade-off between fuel consumption and remaining thrust capability. This is quantified by the thrust margin

$$FN_{margin} = \frac{FN_{max} - FN_{target}}{FN_{target}} \tag{4}$$

where FN_{max} is the maximum thrust available at full-load operation and FN_{target} is the prescribed target thrust. A positive thrust margin indicates that the design retains additional thrust capability above the target condition. Consequently, target-thrust candidates are assessed not only by *TSFC*, but also by propeller diameter, chord ratio plausibility, estimated extension mass and thrust margin.

4.4.1 Geared Target-thrust Designs

For the geared configuration, the target-thrust condition is reached by considering reduced gas-generator power settings N_{rel}. For each part-load gas-generator condition, the modular extension is redesigned for the resulting maximum available thrust, rather than by merely throttling the propeller shaft power of a fixed full-load design. This reduces fuel flow and the power available to the power

turbine, so that the propulsion system operates at a part-load condition corresponding to FN_{target} = 1000 N. The gearbox does not define the thrust setting itself, but provides an additional degree of freedom for matching propeller and power turbine speed when selecting a target-thrust-adapted design.

Figure 5 shows the geared-drive candidates evaluated at FN_{target} = 1000 N as a function of propeller diameter and *TSFC*. The grey points represent the investigated candidates, while the blue line indicates the minimum-*TSFC* envelope over propeller diameter. The red line represents the full-load reference corridor introduced in Section 4.2 and illustrates how a full-load-oriented design compares with target-thrust-adapted candidates.

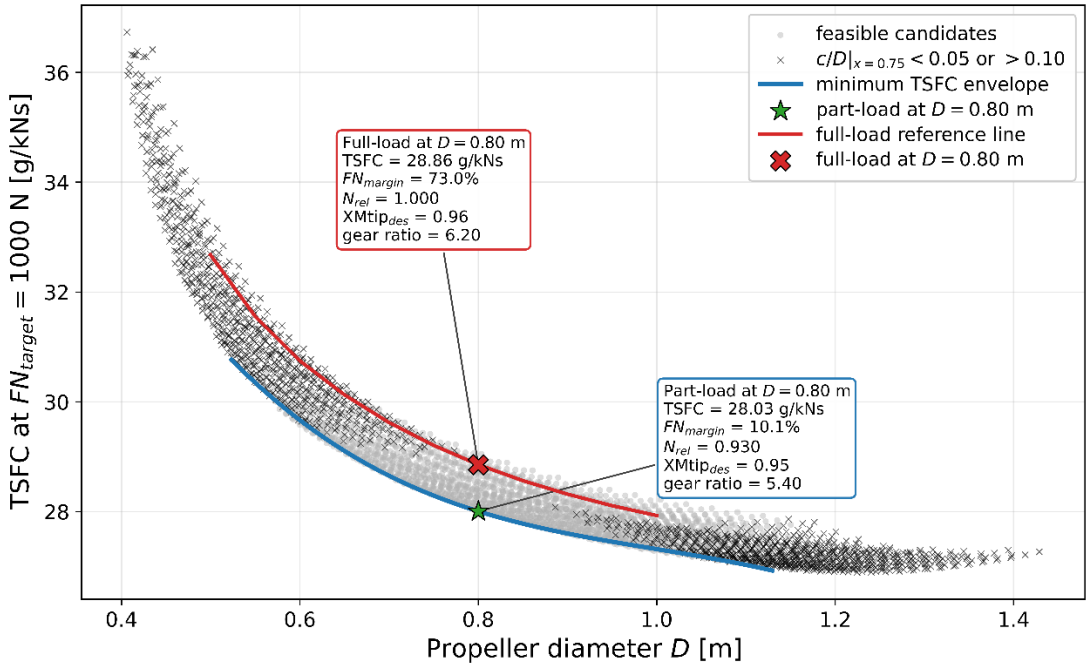


Figure 5 – Geared-drive configuration: target-thrust design potential for FN_{target} = 1000 N.

The target-thrust-adapted envelope lies below the full-load reference over a wide range of propeller diameters. This shows that a design selected for maximum available thrust is not necessarily the most fuel-efficient choice for a required target-thrust. At a given diameter, *TSFC* can be reduced by selecting a design that better matches the part-load operating condition of the gas generator, power turbine and propeller. In the geared architecture, the gearbox helps preserve favorable speed matching between power turbine and propeller over this adapted operating range.

At the representative diameter D = 0.8 m the target-thrust-adapted candidate therefore achieves a lower *TSFC* than the corresponding full-load reference design. This improvement is obtained at the cost of a reduced thrust margin, since the design is no longer selected primarily for maximum thrust capability. The result illustrates the system-level trade-off between fuel consumption at a specified operating point and remaining thrust capability above this target condition.

The diameter trend indicates that larger propellers generally reduce *TSFC* at the target-thrust condition by lowering disk loading and improving propeller efficiency. However, this benefit must be balanced against installation constraints and estimated extension mass. The minimum-*TSFC* envelope should therefore not be interpreted as a recommendation to maximize propeller diameter, but as a basis for selecting the best candidate under a given diameter constraint.

As in the full-load design space, the chord ratio criterion remains a plausibility check for the propeller geometry. Some small-diameter candidates would require a modified propeller layout, for example through a different blade number or loading distribution. The target-thrust study therefore identifies promising operating regions, while the final propeller layout remains a subsequent aerodynamic design task.

4.4.2 Direct Target-thrust Designs

The direct-drive target-thrust study follows the same basic approach as the geared case: the prescribed target thrust is primarily reached by reducing the gas-generator power setting N_{rel}. However, the available design mechanisms differ substantially. Since no gearbox is available, propeller and power turbine speed remain directly coupled. Consequently, the selection of a target-thrust-adapted design depends more strongly on the combined variation of gas-generator load, design tip Mach number and remaining nozzle pressure ratio.

Figure 6 shows the direct-drive candidates evaluated at FN_{target} = 1000 N. The full-load reference design is included as a comparison point, while the target-thrust-adapted minimum indicates the best candidate within the investigated parameter range and constraints. In contrast to the geared architecture, the candidate distribution is more compact and more strongly constrained by the feasible diameter and chord ratio range.

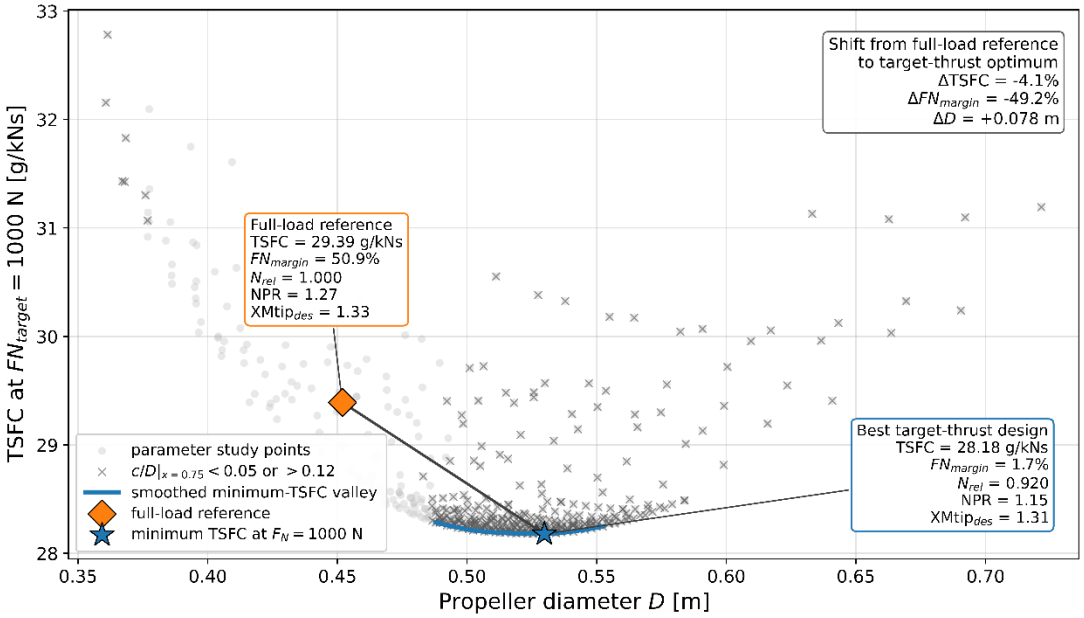


Figure 6 – Direct-drive configuration: target-thrust design potential for FN_{target} = 1000 N.

The results indicate that the direct-drive configuration can also reduce *TSFC* at the target-thrust condition compared with the full-load reference design. This improvement is obtained by selecting a design point that better matches the part-load operating condition of the coupled gas generator, power turbine and propeller. However, the improvement is achieved at the cost of a significantly reduced thrust margin. The best target-thrust candidate is therefore not necessarily a generally preferable design, but rather a design optimized for the specified operating requirement.

The target-thrust optimum is governed by the same coupling mechanisms identified in the full-load design space. Reducing the gas-generator load lowers the available turbine power, while the remaining nozzle pressure ratio influences how the available energy is distributed between shaft power and residual jet thrust. The resulting optimum is therefore a compromise between propeller efficiency, shaft power extraction, residual jet thrust and geometric feasibility.

Compared with the geared configuration, the direct-drive architecture has less freedom to compensate for an unfavorable propeller operating point. Propeller geometry refinements, such as adapting blade number or loading distribution, can improve individual candidates, but they do not remove the fundamental shaft-speed coupling between power turbine and propeller. The direct-drive target-thrust result therefore supports the interpretation from the full-load design-space analysis: the concept can provide a compact and mechanically simpler solution, but its optimum is more constraint-dependent and less robust than that of the geared configuration.

4.5 Constrained Architecture Comparison

The previous sections analyzed the geared and direct-drive configurations separately. In the following, both architectures are compared under prescribed thrust and installation constraints by selecting the best candidate from the evaluated design set. For each architecture a, target thrust FN_{target}, and maximum allowable propeller diameter D_{max}, the candidate with the lowest *TSFC* at the target

operating point is selected:

$$\min_{x_a} TSFC(x_a)$$

$$\text{s.t.} \quad FN(x_a) = FN_{target}, \quad D(x_a) \le D_{max}, \quad 0.05 \le \frac{c}{D}\Big|_{x=0.75} \le 0.10 \tag{5}$$

$$\text{with} \quad x_{geared} = \left[XM_{tip}, N_{rel}, i_{gear}\right] \text{ and } x_{direct} = \left[XM_{tip}, N_{rel}, NPR\right]$$

and the investigated parameter ranges

$$XM_{tip} \le 1.4, \; 0.8 \le N_{rel} \le 1.0, \; 1.05 \le NPR \le 1.4, \; 2.0 \le i_{gear} \le 9.0$$

The selected candidates are evaluated not only by *TSFC*, but also by propeller diameter, estimated extension mass as defined in Eq. (3), and the thrust margin introduced in Eq. (4).

It is important to emphasize that this comparison is not intended to identify a universally superior architecture. Although both configurations are evaluated for the same target thrust levels and diameter constraints, they do not represent a fully symmetric design problem. The geared configuration exploits the gearbox degree of freedom to decouple power turbine and propeller speed. The direct-drive configuration, in contrast, has to compensate for the missing gearbox degree of freedom by adapting the remaining nozzle pressure ratio and by relying on a more aggressive high-speed propeller parametrization, including higher sweep and high blade-tip Mach numbers. The comparison therefore reflects the performance of two architecture-specific design strategies under a common set of target-thrust and diameter constraints, rather than a general evaluation of the two architectures.

The constrained optimization procedure is illustrated in Figure 7 for the representative case of FN_{target} = 1000 N and D_{max} = 0.8 m. The figure shows the feasible and infeasible candidates of both architectures in the *TSFC*-diameter plane. For the geared configuration, the full-load reference line is included together with the target-thrust-adapted candidates. For the direct-drive configuration, the evaluated candidates form a more compact region at smaller propeller diameters. The marked optima therefore represent the best candidates under the prescribed target thrust, diameter constraint and chord ratio criterion, rather than unconstrained architecture optima.

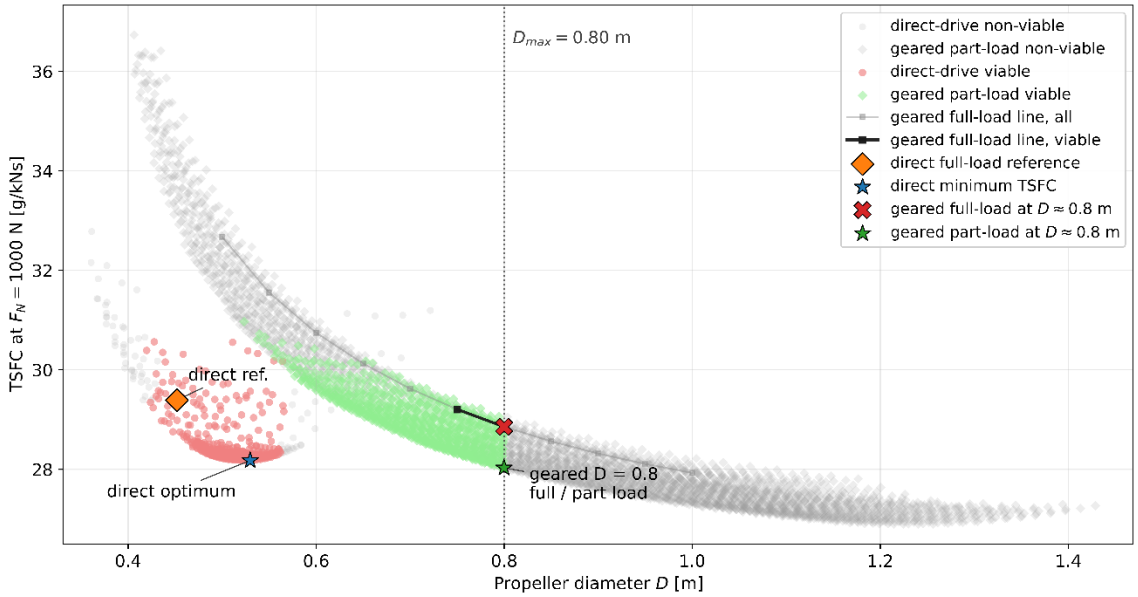


Figure 7 – Direct-drive and geared configuration: target-thrust design potential for FN_{target} = 1000 N, D_{max} = 0.8 m, $c/D|_{x=0.75}$ = 0.05 – 0.1.

For this specific case, the geared-drive optimum achieves the lowest *TSFC* within the evaluated design set, while the direct-drive target-thrust candidate remains slightly above it. At the same time, Figure 7 illustrates the different design mechanisms of the two architectures. The geared configuration follows a diameter-dependent design corridor and benefits from increasing propeller diameter,

whereas the direct-drive candidates remain governed by the compact high-speed propeller strategy.

The same constrained optimization was then applied to additional target thrust levels and diameter constraints. The resulting candidates are summarized in Table 3.

Table 3 – Selected candidates for different target-thrust levels and diameter constraints

FN_{target} [N]	D_{max} [m]	D [m]	$TSFC$ @ FN_{target} [g/kNs]	Design Parameters* [–]	B [–]	FN_{margin} [%]
Geared-drive						
600	0.6	0.6	36.21	XM_{tip} = 0.925, N_{rel} = 0.91, i_{gear} = 4.0	8	47.7
600	0.8	0.8	34.70	XM_{tip} = 0.915, N_{rel} = 0.91, i_{gear} = 5.4	8	59.7
600	1.0	1.0	34.08	XM_{tip} = 0.89, N_{rel} = 0.91, i_{gear} = 7.0	6	65.2
1000	0.6	0.6	29.71	XM_{tip} = 1.02, N_{rel} = 0.93, i_{gear} = 3.7	8	0.7
1000	0.8	0.8	28.03	XM_{tip} = 0.95, N_{rel} = 0.93, i_{gear} = 5.4	8	10.1**
1000	1.0	1.0	27.37	XM_{tip} = 0.93, N_{rel} = 0.93, i_{gear} = 6.9	6	14.2
1400	0.6	0.6	26.95	XM_{tip} = 0.99, N_{rel} = 0.98, i_{gear} = 4.3	10	0.3
1400	0.8	0.8	25.45	XM_{tip} = 0.995, N_{rel} = 0.98, i_{gear} = 5.7	6	8.5
1400	1.0	1.0	24.48	XM_{tip} = 0.93, N_{rel} = 0.975, i_{gear} = 7.6	6	10.6
Direct-drive						
600	0.6	0.590	32.83	XM_{tip} = 1.32, N_{rel} = 0.89, NPR = 1.14	5	41.1
1000	0.6	0.526	28.18	XM_{tip} = 1.315, N_{rel} = 0.925, NPR = 1.155	6	1.7**
1400	0.6	0.484	27.57	XM_{tip} = 1.35, N_{rel} = 0.985, NPR = 1.265	6	0.4

***** Design parameters given for design point @ FN_{max}

****** compared in Figure 7

The table shows that the direct-drive configuration can be competitive under strict diameter constraints and especially at lower target thrust levels. This behavior results from the selected compact-diameter design strategy, which combines high blade-tip Mach numbers, increased sweep and variation of the remaining nozzle pressure ratio in order to compensate for the missing gearbox degree of freedom. However, this should not be interpreted as a generally dominant direct-drive architecture. The comparison is based on architecture-specific assumptions and does not represent a fully symmetric design problem: the geared configuration uses the gearbox to decouple power turbine and propeller speed and therefore provides a broader design corridor, whereas the direct-drive configuration relies on a more aggressive high-speed propeller parametrization and direct shaft-speed coupling. A geared configuration using similarly aggressive propeller assumptions was not investigated here and could improve the performance of geared candidates at smaller diameters, thereby reducing the apparent gap to the direct-drive configuration under compact-diameter constraints.

The geared configuration shows a different scaling behavior. For small maximum diameters, the gearbox degree of freedom cannot fully compensate for the efficiency penalties associated with generating the required thrust on a limited propeller disk area. As the allowable diameter is increased, however, the geared configuration benefits more strongly from the additional propeller disk area. The gearbox allows the propeller to be operated closer to an aerodynamically favorable speed range while maintaining suitable power turbine conditions. Consequently, the geared-drive candidates show a continuous improvement with increasing D_{max} and become increasingly attractive when larger installation diameters are acceptable. This trend becomes more relevant at higher target thrust levels, where the benefit of lower disk loading and favorable propeller efficiency increases.

In addition, the apparent compactness advantage of the direct-drive configuration remains subject to considerable uncertainty at this conceptual design stage. Although eliminating the gearbox reduces one major component, the resulting architecture may introduce additional challenges related to mechanical complexity, extension mass, blade stresses, bearing arrangement, axial length, structural integration, aeroelastic behavior, and vibration. These aspects are not yet captured with sufficient fidelity in the present assessment. The direct-drive results should therefore be understood as an indication of potential under the selected assumptions, but require further aerodynamic, structural and integration studies before the concept can be considered technically substantiated.

Overall, the constrained comparison confirms the interpretation derived from the individual design-space analyses. The geared architecture provides a broader and more robust design space due to

shaft-speed decoupling, but introduces additional gearbox mass and integration complexity. The direct-drive architecture eliminates the gearbox and can be competitive for compact configurations, but its performance depends strongly on the assumed feasibility of highly swept, high-tip-Mach-number propellers, the selected turbine parametrization and the unresolved integration challenges mentioned above. The results should therefore be interpreted as a comparison of architecture-specific conceptual design strategies under the assumptions of this study, rather than as a final assessment of one architecture being generally superior to the other.

5. Conclusion and Outlook

This paper presented an integrated conceptual design process for the MOJO turboprop extension and applied it to geared and direct-drive configurations. The results show that the geared configuration benefits from speed decoupling and provides a robust design corridor over a wide range of propeller diameters. Larger diameters improve propeller efficiency and fuel consumption potential, but introduce installation and mass penalties.

The direct-drive configuration avoids the gearbox and may provide a compact solution, but its design space is more strongly constrained by the fixed shaft-speed coupling between power turbine and propeller. Its optimum therefore depends more sensitively on tip Mach number, nozzle pressure ratio, turbine loading and propeller geometry assumptions. The constrained comparison further indicates that direct-drive competitiveness is mainly observed under compact-diameter requirements and relies on aggressive high-speed propeller assumptions, which still require further aerodynamic, structural and integration assessment.

Target-thrust studies, in which the modular extension is adapted to reduced gas-generator power settings for a prescribed thrust requirement, show that candidates selected from the full-load design space are not necessarily the most fuel-efficient designs at lower required thrust levels. Fuel consumption improvements at the target condition must be evaluated together with the resulting reduction in thrust margin. Future work will extend the constrained optimization toward additional thrust levels and platform-level installation and mission constraints.

6. Contact Author Email Address

Tomasz.Matuschek@dlr.de

7. Copyright Statement

The authors confirm that they, and/or their company or organization, hold copyright on all of the original material included in this paper. The authors also confirm that they have obtained permission, from the copyright holder of any third party material included in this paper, to publish it as part of their paper. The authors confirm that they give permission, or have obtained permission from the copyright holder of this paper, for the publication and distribution of this paper as part of the ICAS proceedings or as individual off-prints from the proceedings.

References

[1] Zhang B.; Song Z.; Zhao F. and Liu C. Overview of Propulsion Systems for Unmanned Aerial Vehicles. *Energies 2022*, 15(2), 455, 2022

[2] Matuschek T., Otten T., Häßy J., Frank J., Brakmann R. Modular Jet and Propeller Engine – Part I: Initial Studies, *35th Congress of the International Council of the Aeronautical Sciences*, Sydney (Australia), ICAS2026_0813, 2026

[3] Reitenbach S. et al. Collaborative Aircraft Engine Preliminary Design using a Virtual Engine Platform, Part A: Architecture and Methodology. *AIAA SciTech 2020 Forum*, Orlando (Florida), 2020

[4] Institute of Propulsion Technology, German Aerospace Center (DLR). GTlab - Gas Turbine Laboratory. https://www.gtlab.de/

[5] Häßy J. Validierung und Implementierung eines Verfahrens zur Vorauslegung von Propellern auf Basis der Blattelementtheorie, Bachelor thesis, RWTH Aachen, 2016

[6] Häßy J. Untersuchung zum Einfluss des Propellers im Gesamtkontext der Triebwerksvorauslegung, Master thesis, RWTH Aachen, 2018

[7] Häßy J., Bolemant M. and Becker R. G. An Educated Guess - Predicting Turbomachinery Efficiencies of Aero Engines During Conceptual Design. *ASME Turbo Expo 2023: Power for Land, Sea, and Air*, Boston, 2023

[8] Kost F. Ein Verfahren zur Berechnung der Meridionalströmung von Axialturbinen (DLR-IB 225-2014). DLR-Internal Report, 2014.

[9] Krumme K. Performance Prediction and Early Design Code for Axial Turbines and its Application in Research and Predesign. *Proceedings of the ASME Turbo Expo 2016*, Seoul, South Korea, 2016

[10] Grunwitz C., Nelles D., Carvalho F., Schöffler R., Brose N., Wehrel P. A Comprehensive Multifidelity Design and Analysis Process for Cooled Axial Flow Turbines: From Concept to Component, *Proceedings of IGTC 2023*, Kyoto, Japan, 2023

[11] Häßy J. and Schmeink J. Knowledge-Based Conceptual Design Methods for Geometry and Mass Estimation of Rubber Aero Engines. *33rd Congress of the International Council of the Aeronautical Sciences*, Stockholm, 2022

[12] Grieb H., *Projektierung von Turboflugtriebwerken*., Springer-Verlag, 2013.

[13] Strack W. C. et al. *Technology and Benefits of Aircraft Counter Rotation Propellers*. NASA Technical Memorandum, NASA-TM-82983, 1982

[14] Wehrel P. et al. Conceptual Performance and Mass Assessment of an Open Fan Engine for a Short-Medium Range Aircraft. *35th Congress of the International Council of the Aeronautical Sciences*, Sydney (Australia), ICAS2026_0261, 2026

[15] Rohrbach C., Metzger F. B., Black D. M., Ladden R.M., Evaluation of Wind Tunnel Performance Testings of an Advanced 45 Degree Swept Eight-Bladed Propeller at Mach Numbers from 0.45 to 0.85, NASA CR-3505, 1982

[16] Jeracki R. J., Mikkelson D. C. and Blaha B. J. Wind Tunnel Performance of Four Energy Efficient Propellers Designed for Mach 0.8 Cruise. NASA Technical Memorandum 79124, Lewis Research Center, 1979.